

# Quantitative and Semiquantitative Bone Erosion Assessment on High-resolution Peripheral Quantitative Computed Tomography in Rheumatoid Arthritis

Waraporn Srikhum, Warapat Virayavanich, Andrew J. Burghardt, Andrew Yu, Thomas M. Link, John B. Imboden, and Xiaojuan Li

**ABSTRACT. Objective.** To develop novel quantitative and semiquantitative bone erosion measures at metacarpophalangeal (MCP) and wrist joints in patients with rheumatoid arthritis (RA) using high-resolution peripheral quantitative computed tomography (HR-pQCT), and to correlate these measurements with disease duration and bone marrow edema (BME) patterns derived from magnetic resonance imaging (MRI).

**Methods.** Sixteen patients with RA and 7 healthy subjects underwent hand and wrist HR-pQCT and 3-Tesla MRI. Bone erosions of the MCP2, MCP3, and distal radius were evaluated by measuring maximal erosion dimension on axial slices, which is a simple and fast measurement, and then were graded (grades 0–3) based on the maximal dimension. Correlation coefficients were calculated between (1) sum maximal dimensions, highest grades, and sum grades of bone erosions; (2) erosion measures and the clinical evaluation; (3) erosion measures and BME volume in distal radius.

**Results.** The inter- and intrareader agreements of maximal erosion dimensions were excellent (intra-class correlation coefficients 0.89, 0.99, and root mean square error 9.4%, 4.7%, respectively). Highest grades and sum grades were significantly correlated to sum maximal dimensions of all erosions. Number of erosions, sum maximal erosion dimensions, highest grades, and sum grades correlated significantly with disease duration. Number of erosions, sum maximal dimensions, and erosion grading of the distal radius correlated significantly with BME volume.

**Conclusion.** HR-pQCT provides a sensitive method with high reader agreement in assessment of structural bone damage in RA. The good correlation of erosion measures with disease duration as well as BME volume suggests that they could become feasible measures of erosions in RA. (First Release Feb 15 2013; J Rheumatol 2013;40:408–16; doi:10.3899/jrheum.120780)

## Key Indexing Terms:

RHEUMATOID ARTHRITIS  
JOINT EROSIONS

DIAGNOSTIC IMAGING

COMPUTED TOMOGRAPHY  
ARTHRITIS

From the Musculoskeletal Quantitative Imaging Research Group, Department of Radiology and Biomedical Imaging, UCSF (University of California, San Francisco), USA.

Supported by a UCSF Radiology Seed Grant and a UCSF Academic Senate Research Grant.

W. Srikhum, MD, Research Fellow, Department of Radiology and Biomedical Imaging, UCSF, Lecturer in Radiology, Faculty of Medicine, Thammasat University, Pathum Thani, Thailand; W. Virayavanich, MD, Research Fellow, Department of Radiology and Biomedical Imaging, UCSF, Lecturer in Radiology, Faculty of Medicine, Ramathibodi Hospital, Mahidol University, Bangkok, Thailand; A. Burghardt, Researcher, Musculoskeletal Quantitative Imaging Research Group, Department of Radiology and Biomedical Imaging, UCSF; A. Yu, Undergraduate Student, Department of Bioengineering, University of California, Berkeley; T. Link, MD, PhD, Professor of Radiology, Chief, Musculoskeletal Imaging and Clinical Director, Musculoskeletal and Quantitative Imaging Research Group, Department of Radiology and Biomedical Imaging, UCSF; J. Imboden, MD, Professor of Rheumatology, Department of Medicine, UCSF, Division of Rheumatology, San Francisco General Hospital; X. Li, PhD, Associate Professor, Department of Radiology and Biomedical Imaging, UCSF.

Address reprint requests to X. Li, Department of Radiology and Biomedical Imaging, UCSF, 185 Berry Street, Suite 350, San Francisco, CA 94107, USA. E-mail: xiaojuan.li@ucsf.edu

Accepted for publication December 19, 2012.

Rheumatoid arthritis (RA), the most common type of inflammatory arthritis, causes chronic inflammation of the synovium and can destroy articular cartilage and erode adjacent bone. Bone erosions are the characteristic of joint damage in RA. The presence of bone erosions at diagnosis and increases in size and number are signs of poor prognosis and aggressive disease<sup>1,2,3,4,5</sup>. A sensitive and reliable imaging technique is important in diagnosis and therapeutic monitoring in patients with RA. Conventional radiographs are currently considered the gold standard for diagnosing and monitoring bone erosion<sup>6,7</sup>. However, radiographs have low sensitivity in detection of bone erosions, particularly in early disease<sup>8,9,10,11,12</sup>. Other imaging methods such as magnetic resonance imaging (MRI) and ultrasonography have demonstrated more sensitivity and accuracy in detection of bone erosions than radiography<sup>8,9,10,11,12,13,14,15,16,17,18,19</sup>. Computed tomography (CT) is more sensitive than radiography or even MRI for detection of bone erosions and can be considered a standard of reference for detection of bone erosions in RA<sup>11,12,13,14,15,19,20,21</sup>.

However, CT has been rarely used in clinical practice because of ionizing radiation exposure.

High-resolution peripheral quantitative CT (HR-pQCT) is a new technique that has been used to assess volumetric bone mineral density at peripheral sites<sup>22,23</sup>. Because of the shorter image acquisition time than for MRI, low radiation dose, and high reproducibility in assessing bony erosions<sup>24</sup>, HR-pQCT is an interesting method for advanced imaging in clinical RA studies. Initial studies using HR-pQCT to evaluate bone microarchitectural impairment and volumetric density as well as bone erosion volume in patients with RA showed promising results<sup>24,25,26</sup>. Our objectives were (1) to assess bone erosions at the metacarpophalangeal (MCP) and wrist joints in patients with RA; (2) to develop reliable quantitative and semiquantitative measures for bone erosions by using HR-pQCT; and (3) to investigate the relationship of these measurements to disease duration and patterns of bone marrow edema (BME) measured using MRI.

## MATERIALS AND METHODS

**Patients.** Sixteen patients with RA who fulfilled the 1987 American College of Rheumatology classification criteria<sup>27</sup> were recruited for this study. All patients had Disease Activity Score 28 (DAS28) measured by experienced faculty rheumatologists at the University of California, San Francisco, in a dedicated RA clinic. Rheumatoid factor (RF) and anti-cyclic citrullinated peptide antibody (anti-CCP Ab) status at diagnosis as well as treatment data including use of disease-modifying antirheumatic drugs (DMARD), prednisone, and tumor necrosis factor (TNF) blocker were collected. All patients underwent HR-pQCT examinations of MCP and proximal wrist joints, and 3-Tesla MRI of the wrist joints. We also studied 7 healthy individuals, who all underwent HR-pQCT examinations of MCP, whereas only 3 healthy subjects underwent HR-pQCT examinations of wrist joints. The study was approved by our institutional review board and informed consent was obtained from each individual.

**HR-pQCT measurements.** All subjects were imaged in a clinical HR-pQCT system (XtremeCT; Scanco Medical AG) at the hand with manifest disease (RA subjects) or on the dominant side (healthy controls). To minimize radiation dose and scan time, separate acquisitions were performed for the wrist and MCP sites. For the MCP acquisition, the subject's forearm was fixed in a palm-down orientation within a custom carbon-fiber cast designed at our institution. The wrist acquisition was performed in the standard forearm cast provided by the manufacturer with the hand in a thumb-up orientation<sup>28</sup>. A single dorsal-palmar projection image of the hand/wrist was acquired to define the tomographic scan region for each site. For the MCP, this region was centered at the apex of the second MCP and extended 13.53 mm in the distal and proximal directions (330 slices total). For the wrist, the midpoint of the radial endplate was used as anatomical reference position with the scan region extending 8.54 mm in the distal direction and 18.52 mm in the proximal direction (330 slices total). The wrist positions were selected such that the most proximal 110 slices corresponded to the standard location (9.5 mm proximal to the midpoint of the radial endplate) for imaging bone quality described in the osteoporosis literature<sup>22,23</sup>. For each tomographic acquisition, 750 projections were acquired over 180° with a 100 ms integration time at each angular position. At each site, 3 sequential tomographic acquisitions were required to cover the 27.06 mm length (330 slices) along the supero-inferior axis. The 12.6 cm field of view was reconstructed across a 1536 × 1536 matrix using a modified Feldkamp algorithm, yielding 82-μm voxels<sup>29</sup>. Total scan time was 8.2 min with an effective dose of approximately 12.6 μSv for each site.

**Bone erosion measurement.** Bone erosions of the second and third metacarpal heads (MCP2 and MCP3) and distal radius were evaluated in this cross-sectional study by measuring maximal erosion dimension on axial 2-dimensional (2-D) slices by 2 radiologists independently (WS and WV) as shown in Figure 1. The radiologists were blinded to the clinical data and previous radiology report. Erosions were defined as sharply demarcated juxtaarticular focal bone lesions with a cortical break (loss of cortex) in at least 2 adjacent slices. In addition, questionable cortical break lesions were confirmed by using 3-D images reconstructed by open source Digital Imaging and Communication in Medicine (DICOM) OsiriX software (a free DICOM viewer for Apple computers that could be downloaded from [www.osirix-viewer.com](http://www.osirix-viewer.com)). Measurements of maximal dimension of all erosions were performed twice with a 4-week interval. To simplify quantitative measures for clinical applications, bone erosions in each MCP and distal radius were then semiquantitatively scored according to 4 grades (grades 0–3) based on the maximal dimension of the cortical break, as shown in Figure 2. The highest and sum erosion grades of each site and all regions were analyzed to test a potential measure for clinical use.

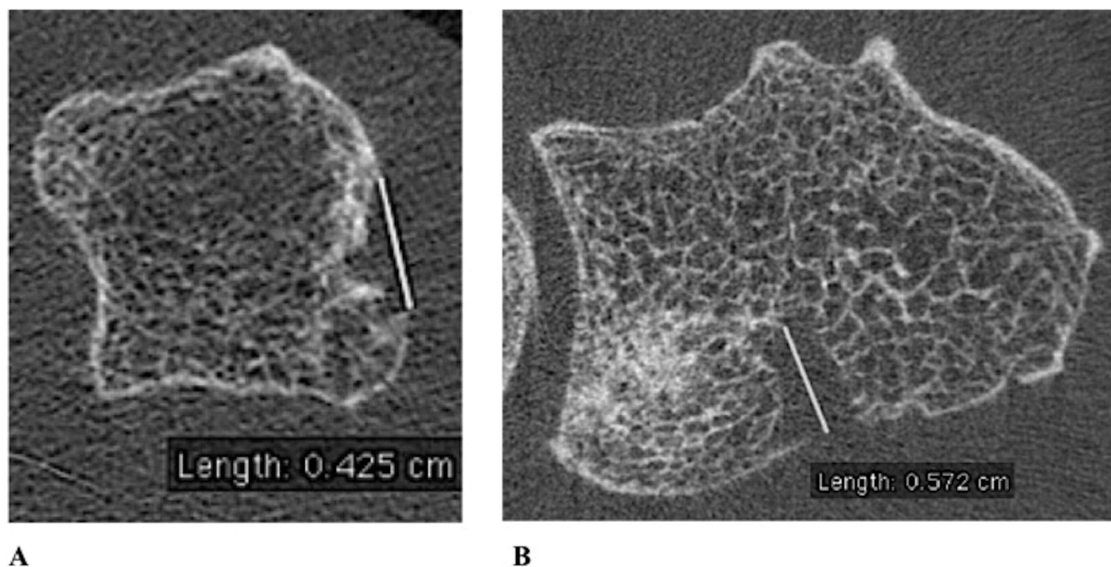
In addition, the time required for the readers to evaluate the images using quantitative erosion measures for each patient at the MCP and distal radius were recorded. Timing comprised the interval from opening the images on the computer screen to completion of measurement of maximal erosion dimensions.

**MRI measurement.** MR images were obtained on a 3-T MR unit (Signa HDx; GE Healthcare) with an 8-channel phased array wrist coil. Patients were in supine position with arms resting on the side of the body. An advanced water/fat separation imaging technique using iterative decomposition of water and fat with echo asymmetry and least-squares estimation (IDEAL) sequences was applied in this study. IDEAL fast-spin echo sequences were used in our previous study<sup>30</sup>, and demonstrated superior bone marrow fat suppression and improved visualization and quantification of the BME compared to conventional fast-spin echo sequences. Coronal and axial T2-weighted IDEAL fast-spin echo sequences (TR/TE = 3500/50 ms, in-plane resolution = 0.2 mm, slice thickness = 2 mm) were obtained and used for image analysis.

**BME volume measurement.** BME pattern was identified by 2 radiologists (WS and WV) independently on the T2-weighted IDEAL fast-spin echo water images after an interval of 4 weeks from the HR-pQCT reading to prevent recall bias. The BME pattern identified was then semiautomatically segmented using an algorithm as reported<sup>31</sup>. Five times SD of signal intensity within normal bone marrow was used as the threshold to automatically segment BME using software developed in-house based on interactive data language (Exelis Visual Information Solutions Inc.). BME volumes were quantified from the 3-D BME contour generated from this process.

**Statistical analysis.** Descriptive statistics (mean, median, range, SD) of quantitative erosion measures were compared between the patients with RA and healthy subjects. To achieve a reliable method for semiquantitative scoring, receiver-operating characteristic (ROC) curve analysis and Youden index were calculated from different summation of maximal dimension erosion measures (2.5–3.5 mm at the MCP) to obtain the best cutoff values for distinguishing healthy subjects from patients with RA. Therefore, the patients with RA were considered abnormal and the control subjects healthy. The highest Youden index was used as a cutoff value between grade 1 and 2 of the semiquantitative grades. Comparative descriptions of the erosion grade between patients and healthy subjects were derived.

For assessment of interreader and intrareader reliability of erosion measures, intraclass correlation coefficient (ICC), root mean square error (RMSE), and Bland-Altman plots were obtained. Spearman correlation coefficients were calculated to study the relationship between sum maximal dimension of bone erosion measures and semiquantitative erosion assessment by using highest grades and sum grades. The relationships between measurements (sum maximal dimensions, highest grades, sum



**A** **B**  
 Figure 1. Axial high-resolution peripheral quantitative computed tomography images (82  $\mu$ m isotropic resolution) of metacarpal head (A) and distal radius (B) of patients with rheumatoid arthritis show evidence of sharply demarcated focal bone lesions with a cortical break representing bone erosions. A single measurement in the maximal dimension of the bone erosions was also obtained.

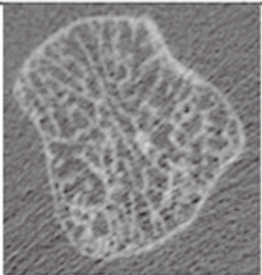
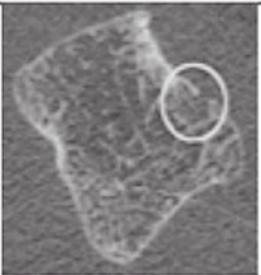
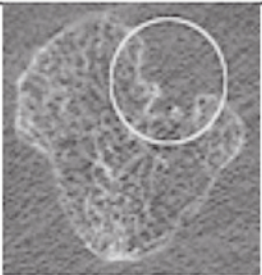
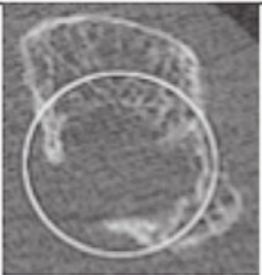
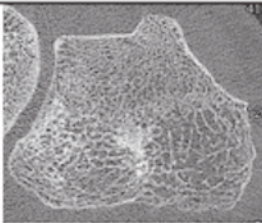
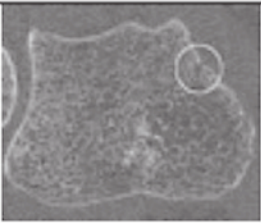
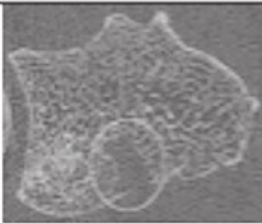
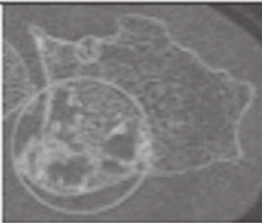
	Grade 0	Grade 1	Grade 2	Grade 3
<b>Metacarpal head erosions</b>				
<b>Definition of erosion grading at MCPs</b>	No evidence of erosion	1 or more erosions with sum maximal dimension < 3.5 mm	1 or more erosions with sum maximal dimension $\geq 3.5$ and $\leq 10$ mm	1 or more erosions with sum maximal dimension > 10 mm
<b>Distal radius erosions</b>				
<b>Definition of erosion grading at distal radius</b>	No evidence of erosions	1 or more erosions with sum maximal dimension < 5 mm	1 or more erosions with sum maximal dimension $\geq 5$ and $\leq 15$ mm	1 or more erosions with sum maximal dimension > 15 mm

Figure 2. Axial high-resolution peripheral quantitative computed tomography images of the metacarpal heads and distal radius of patients with rheumatoid arthritis with different dimensions of erosions and definitions of the semiquantitative grades for evaluating bone erosions at each region. MCP: metacarpophalangeal.



grades, and number of erosions) and the clinical evaluation [disease duration, erythrocyte sedimentation rate (ESR), C-reactive protein (CRP), DAS28-ESR, and DAS28-CRP] were assessed by calculating Spearman correlation coefficients. Spearman correlation coefficients were also used to analyze the correlation between cross-sectional erosion measures in the distal radius and BME pattern volume.

The statistical significance level was set at 0.01 and all statistical analyses were performed on Stata software version 11.1 for Mac.

RESULTS

We studied 16 patients with RA (13 women, 3 men) with mean disease duration 7.7 ± 7.6 years (range 14–302 months). Thirteen patients were positive for RF and ACPA. The mean ESR, CRP, DAS28-ESR, and DAS28-CRP were 22.9 ± 25.1 mm/h, 5 ± 5.2 mg/dl, 3.7 ± 1.5, and 3.5 ± 1.4, respectively. Fifteen, 10, and 6 patients were treated with DMARD, prednisone, and TNF blocker, respectively (Table 1). In addition, 7 healthy female subjects with mean age 50.1 ± 15.0 years were studied.

Thirty, 8, and 26 erosions were found at MCP2, MCP3, and distal radius in 11, 8, and 10 patients, respectively. Five patients had erosions at all of these sites. The mean maximal dimensions of erosions at the MCP2, MCP3, and distal radius were 0.40 ± 0.22 cm, 0.32 ± 0.21 cm, and 0.46 ± 0.31 cm, respectively, and ranged from 0.12 to 0.88 cm at the MCP and from 0.10 to 1.34 cm at the distal radius. In healthy individuals, 3 erosions were found at the MCP2 and MCP3 in 2 and 3 subjects and 1 erosion was found at the distal radius. The mean maximal erosion dimensions of the healthy subjects were 0.26 ± 0.08 cm and 0.29 ± 0.05 cm at

the MCP2 and MCP3, respectively (range 0.18–0.34 cm). The maximal erosion dimension at the distal radius was 0.13 cm. The inter- and intrareader agreements of maximal erosion dimension measurements were excellent (ICC 0.89 and 0.99 and RMSE 9.4% and 4.7%, respectively). Bland-Altman plots illustrating the inter- and intrareader reproducibility are shown in Figure 3.

ROC curve and Youden index of the different cutoff values were analyzed for developing reliable semiquantitative grades as defined. A summation of maximal dimension value < 3.5 mm at the MCP showed the best capability in distinguishing healthy subjects from the patients with RA, with a Youden index of 0.54, sensitivity 0.69, and specificity 0.86. Only 1 erosion was detected at the distal radius in a healthy subject. We therefore considered a summation of the maximal dimension < 5 mm as a cutoff value between grade 1 and 2 of the semiquantitative grades at the distal radius. The median grades of MCP2, MCP3, and distal radius of the patient group were 2, 0.5, and 1, respectively, whereas the median grades of the healthy subjects were 0 at all sites.

The highest grades and sum grades of all erosions were strongly correlated with sum maximal dimensions (r = 0.91 and r = 0.92, both p < 0.01, respectively). There were also highly significant correlations between the MCP and distal radius grades and the highest and sum grades of all erosions (r = 0.87 and r = 0.89 at the MCP and r = 0.77 and r = 0.80 at the distal radius, p < 0.01; Table 2).

The number of erosions, sum maximal erosion dimensions, highest grades, and sum grades of all erosions as well as sum maximal dimensions and highest grades of the MCP showed significant correlation with disease duration (r = 0.66–0.75, p < 0.01), but not with ESR, CRP, DAS28-ESR, and DAS28-CRP (Table 3).

From 7 patients, 20 out of 26 erosions (76.9%) in the radius identified with HR-pQCT were also identified in MR images. All these 20 erosions were found to be surrounded by BME pattern, and the other 6 erosions had no obvious BME pattern in MR images. The mean BME volume was 0.65 ± 0.90 cm<sup>3</sup>. The number of erosions, sum maximal dimensions, and erosion grading of the distal radius correlated significantly with quantification of BME volume (r = 0.86, r = 0.90, r = 0.89, respectively; p < 0.01). Examples of patient images are shown in Figure 4.

The median times per patient for quantitative erosion measures at the MCP and distal radius were 2 min (range 1.20–5.30 min) and 1.48 min (range 1.15–4.50 min), respectively.

DISCUSSION

HR-pQCT has recently received attention as a novel imaging modality for RA because of its high spatial resolution and significant reduction of the radiation dose compared to standard multidetector CT (MDCT).

Table 1. Patient characteristics.

Characteristics	All Patients, n = 16
Sex, no. female (%)	13 (81)
Age, yrs, mean ± SD	52.9 ± 12.7
Ethnicity, n (%)	
Latino/Hispanic	8 (50)
Asian/Pacific Islander	3 (19)
White	5 (31)
Disease duration, yrs, mean ± SD	7.6 ± 7.1
DAS28-ESR*, mean ± SD	3.7 ± 1.5
DAS28-CRP*, mean ± SD	3.5 ± 1.4
ESR, mm/h, mean ± SD	22.9 ± 25.1
CRP, mg/dl, mean ± SD	5.0 ± 5.2
RF-positive, n (%)	13 (81)
Anti-CCP Ab-positive, n (%)	13 (81)
DMARD†, n (%)	15 (94)
Methotrexate, n (%)	12 (75)
Prednisone, n (%)	10 (63)
Anti-TNF, n (%)	6 (38)

\* Disease Activity Scale (DAS)28 is calculated using tender and swollen joint counts, patient global visual analog scale, and erythrocyte sedimentation rate (ESR) or C-reactive protein (CRP). † Any disease-modifying antirheumatic drug (DMARD) other than prednisone (methotrexate, plaquenil, sulfasalazine, azathioprine, leflunomide, anti-tumor necrosis factor-α medications, and rituximab). RF: rheumatoid factor; Anti-CCP Ab: anticitrullinated protein antibodies; TNF: tumor necrosis factor.

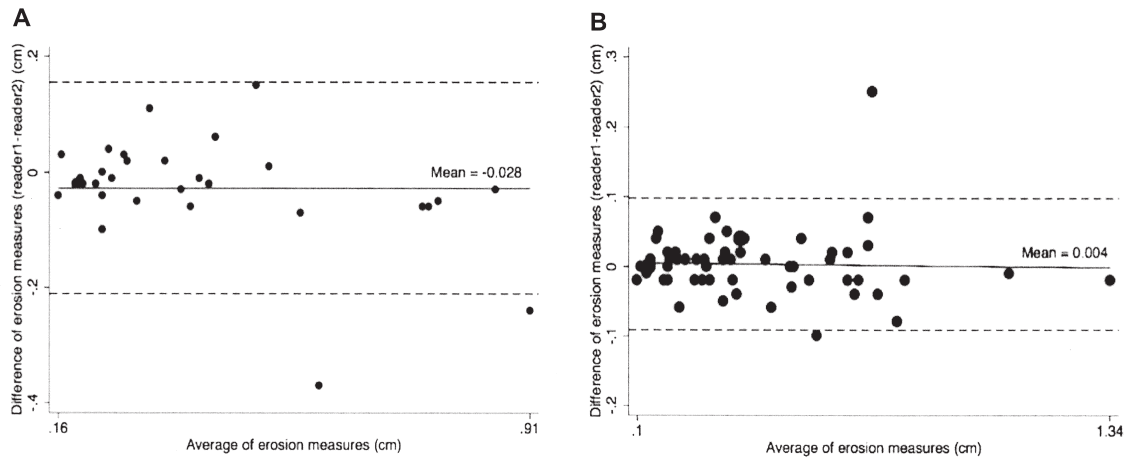


Figure 3. Bland-Altman plots show interreader (A) and intrareader (B) agreement of bone erosion measurements using maximal erosion dimension. Solid line indicates the mean absolute difference, broken lines represent 95% limits of agreement.

Table 2. Correlation analyses of quantitative and semiquantitative bone erosion measures: table shows Spearman correlation coefficients (first row) and 2-tailed p values (second row).

	Sum Grade of All Erosions	Highest Grade of All Erosions	Sum Maximal Dimension of All Erosions	Total No. Erosions	Highest Grade of MCP	Sum Maximal Dimension of MCP	No. Erosions at MCP	Grade of Distal Radius	Sum Maximal Dimension of Distal Radius	No. Erosions at Distal Radius
Sum grade of all erosions	1.0000									
Highest grade of all erosions	0.8895*	1.0000								
Sum maximal dimension of all erosions	0.9238*	0.9115*	1.0000							
Total no. erosions	0.8615*	0.9010*	0.9659*	1.0000						
Highest grade of MCP	0.8929*	0.8676*	0.7920*	0.7895*	1.0000					
Sum maximal dimension of MCP	0.8673*	0.8372*	0.8207*	0.8671*	0.9318*	1.0000				
No. erosions at MCP	0.7811*	0.7702*	0.7938*	0.8665*	0.8619*	0.9565*	1.0000			
Grade of distal radius	0.8047*	0.7684*	0.8705*	0.7716*	0.5538	0.5299	0.4302	1.0000		
Sum maximal dimension of distal radius	0.7919*	0.7511*	0.8704*	0.7798*	0.5331	0.5149	0.4434	0.9858*	1.0000	
No. erosions at distal radius	0.7356*	0.7473*	0.8182*	0.7478*	0.4761	0.4620	0.3578	0.9738*	0.9711*	1.0000

\* Significant correlation,  $p < 0.01$ . MCP: metacarpophalangeal joint.

High-resolution MDCT protocols for assessing bone microarchitecture are typically associated with an effective dose of about 3 mSv compared to only 4–13  $\mu$ Sv with standard HR-pQCT protocols<sup>32</sup>. The HR-pQCT protocol used in our study confirmed this advantage, with an effective dose of roughly 12.6  $\mu$ Sv at each site.

We focused on evaluating the ability of HR-pQCT to assess bone erosions at the MCP and distal radius in patients

with RA. We found that HR-pQCT is a highly sensitive technique to detect small bone erosions, as small as 0.5 mm, as shown in Figure 2 (grade 1). This implied that the HR-pQCT is probably a suitable technique for detecting bone erosions in the early course of disease; this requires confirmation by future longitudinal studies with early RA cohorts. In addition, although it was not an objective of this study, we noted that HR-pQCT can also depict cortical bone

**Table 3.** Correlation analyses of quantitative and semiquantitative bone erosion measures with duration of disease and disease activity; table shows Spearman correlation coefficients (first row) and 2-tailed p values (second row).

	Duration of Disease	ESR	CRP	DAS28-ESR	DAS28-CRP	Sum Grade of All Erosions	Highest Grade of All Erosions	Sum Maximal Dimension of All Erosions	Total no. Erosions	Highest Grade of MCP	Sum Maximal Dimension of MCP
Duration of disease	1.0000										
ESR	-0.2975 0.2815	1.0000									
CRP	-0.2075 0.4580	0.6355 0.0109	1.0000								
DAS28-ESR	-0.0250 0.9295	0.5771 0.0243	0.5993 0.0182	1.0000							
DAS28-CRP	0.0679 0.8101	0.1613 0.5658	0.5367 0.0391	0.8357* 0.0001	1.0000						
Sum grade of all erosions	0.7542* 0.0012	-0.3127 0.2565	-0.3951 0.1449	-0.0601 0.8315	-0.0364 0.8974	1.0000					
Highest grade of all erosions	0.7094* 0.0031	-0.0354 0.9003	-0.2395 0.3899	0.0412 0.8842	-0.0647 0.8189	0.8637* 0.0000	1.0000				
Sum maximal dimension of all erosions	0.7214* 0.0024	-0.0354 0.9003	-0.2395 0.3899	0.0412 0.8842	-0.0647 0.8189	0.9073* 0.0000	0.8916* 0.0000	1.0000			
Total no. erosions	0.7015* 0.0036	-0.0866 0.7588	-0.3937 0.1465	-0.0324 0.9088	-0.0863 0.7597	0.8313* 0.0001	0.8783* 0.0000	0.9587* 0.0000	1.0000		
Highest grade of MCP	0.7387* 0.0017	-0.3462 0.2061	-0.5136 0.0502	-0.2748 0.3215	-0.2963 0.2836	0.8750* 0.0000	0.8481* 0.0001	0.7563* 0.0011	0.7529* 0.0012	1.0000	
Sum maximal dimension of MCP	0.6577* 0.0077	-0.2673 0.3356	-0.6177 0.0141	-0.1859 0.5072	-0.2735 0.3240	0.8452* 0.0001	0.8130* 0.0002	0.8905* 0.0000	0.8497 0.0001	0.9169* 0.0000	1.0000

\* Significant correlation,  $p < 0.01$ . ESR: erythrocyte sedimentation rate; CRP: C-reactive protein; DAS28: Disease Activity Score 28; MCP: metacarpophalangeal joint.

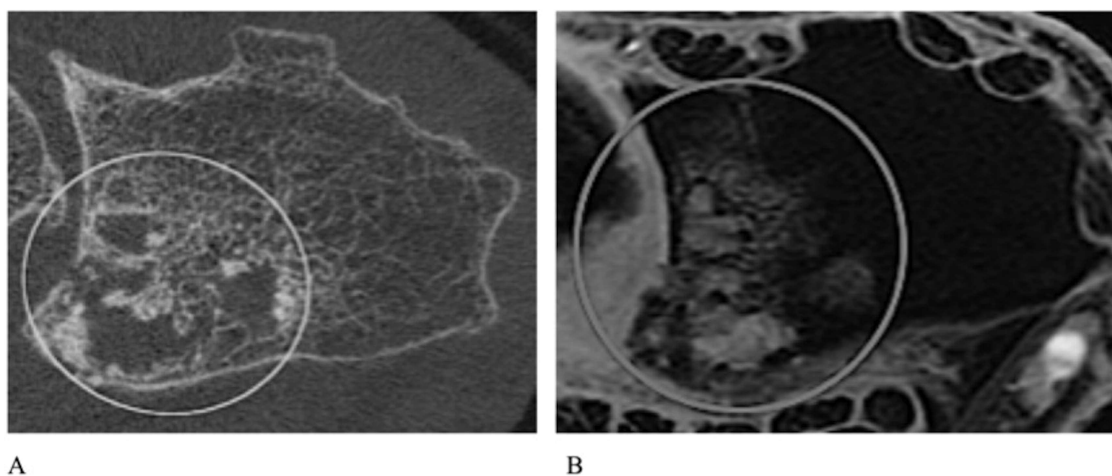


**Figure 4.** Comparative axial high-resolution peripheral quantitative computed tomography (A) and axial T2-weighted fast-spin echo magnetic resonance imaging (MRI) scans using iterative decomposition of water and fat with echo asymmetry and least-squares estimation (IDEAL) sequences (B) of the distal radius in a patient with rheumatoid arthritis; images show extensive erosive changes at the mesial aspect of the radius, visible as a clearly demarcated zone of hyperintense signal within normal hypointense marrow on the MR image. The axial T2-weighted IDEAL fast-spin echo MR image (B) also shows significant patchy hyperintense signal intensity of the bone marrow consistent with edema.

surface irregularity, reactive sclerotic change, osteophytes, or bony proliferation, as observed in a previous HR-pQCT study in RA<sup>25</sup>.

With this novel technique, we developed an applicable quantitative bone erosion measure by using the cumulative maximal erosion dimension in axial slices, which is simpler

and less time-consuming compared to the method using percentage of erosion volume, as proposed by others<sup>24</sup>, and thus would be more straightforward for clinical use, particularly for multiple lesions. Our measure showed excellent intra- and interreader reproducibility. The intraobserver reproducibility in our study was slightly better than that for CT erosion volume measurements (ICC = 0.97), the erosion grading based on HRCT images (ICC = 0.96–0.97)<sup>33</sup>, and the bone erosion subscore of the established Outcome Measures in Rheumatology Clinical Trials RA MRI Scoring (OMERACT RAMRIS) system (ICC = 0.80–0.94)<sup>34,35,36</sup>. The interobserver reliability was also considerably better than that for the OMERACT RAMRIS erosion scoring system (ICC = 0.15–0.85)<sup>35,36,37,38,39</sup>.

Based on the high reliability of measurement of the maximal erosion dimension in 2-D axial slices, we developed a new semiquantitative assessment method using a 4-scale scoring system. The semiquantitative grades were highly correlated to the quantitative measure, suggesting that the novel bone erosion grading is reasonable and potentially applicable for clinical use. Further, when focusing on the erosion grading, the Youden index used as a cutoff value between grades 1 and 2 at the MCP for distinguishing healthy subjects from patients with RA was comparable to that proposed by Stach, *et al*<sup>25</sup> (Youden index = 0.56).

Subsequently we investigated correlation of the novel quantitative and semiquantitative measures with duration of disease and disease activity measures. We found that the number of erosions, sum maximal erosion dimensions, highest grades, and sum grades of all erosions were highly correlated with disease duration, which reflects the accumulation of structural damage during the course of RA. In this cross-sectional analysis, we did not find a statistically significant correlation between either quantitative or semiquantitative measures and disease activity as assessed by ESR, CRP, and DAS28. These results are consistent with the findings of Stach, *et al*<sup>25</sup>, which demonstrated that erosion and osteophyte scores were strongly correlated with disease duration and age, but not disease activity. Interestingly, Fouque-Aubert, *et al*<sup>24</sup> found that volumetric trabecular bone mineral density, as quantified by HR-pQCT, was moderately correlated with disease activity as measured by ESR, CRP, and DAS28. This suggests that trabecular bone components could be more dynamic and indicative of ongoing disease activity.

In addition, as the sum maximal dimensions and grades of only MCP showed significant correlation with disease duration, representing quantitative and semiquantitative measures of all erosions (MCP and radius), we can assume that assessment of only the MCP can be considered representative in evaluation of the disease course if imaging of the wrist joint is not available.

We also examined the correlation between erosion

measures from HR-pQCT (both quantitative and semiquantitative) and BME pattern volume measured in MR images. The BME pattern in RA is due to replacement of bone marrow fat by inflammatory infiltrates<sup>40</sup>, which has been suggested as a potential predictor of radiographic progression in many studies<sup>41,42,43,44</sup>. We have developed semiautomatic quantification techniques for calculating BME pattern volume, which showed excellent reproducibility in our previous study<sup>30</sup>. In this study, we demonstrated a significant correlation between the number of erosions, sum maximal erosion dimensions, and developed erosion grades of the distal radius and quantitative BME volume. When we examined the MR images in detail, all erosions corresponded spatially to clearly demarcated regions of hyperintense signal surrounded by patchy regions of bone marrow edema pattern with hyperintense signal intensity, as shown in Figure 4. Six erosions observed in the HR-pQCT scans were not detected in the MRI scans: these erosions were 0.9–1.7 mm in their maximal dimension. A possible explanation is that there is a gap between each MRI slice, thus the small erosions could be overlooked. It would be interesting to evaluate the diagnostic value of the HR-pQCT scans compared to the widely used MR images in a large-scale study, and to investigate a longitudinal change in bone damage within regions of BME pattern, to examine whether the BME pattern presents a high risk for development of local erosions.

Our study has several limitations. The sample size was small; our results need to be evaluated in larger studies. The semiquantitative and quantitative measures were 2-D and were measured manually, and therefore do not account for the complete 3-D geometry of the lesion; subjective demarcation of the erosion boundary is required, which may be difficult to determine in some cases. Both quantitative measures and the semiquantitative scoring system were developed for the first time and they need to be validated for clinical use in patients with RA. Additionally, there are currently a limited number of HR-pQCT devices, which are primarily located at major research institutions; as well, they require longer scan times compared to conventional MDCT scans.

We demonstrated that HR-pQCT allows sensitive and highly reproducible evaluation of structural bone erosions in patients with RA, and this could become an alternative method in bone-specific evaluation. The high reproducibility and good correlation of these quantitative bone erosion measures and semiquantitative bone erosion scoring system with duration of disease and with BME volume, as potential predictors of radiographic progression, make them potentially valuable methods in longitudinal studies; they could become feasible bone erosion measures for very detailed evaluation of disease course, which is required for analysis of new pharmaceutical treatments.



## ACKNOWLEDGMENT

The authors thank Piyawan Srikhum, Doctoral Student, CEREG-University Paris-Dauphine, for assistance with the statistical analyses.

## REFERENCES

1. Dixey J, Solymosy C, Young A. Is it possible to predict radiological damage in early rheumatoid arthritis (RA)? A report on the occurrence, progression, and prognostic factors of radiological erosions over the first 3 years in 866 patients from the Early RA Study (ERAS). *J Rheumatol Suppl.* 2004 Mar;69:48-54.
2. van der Heijde DM. Radiographic imaging: The 'gold standard' for assessment of disease progression in rheumatoid arthritis. *Rheumatology* 2000;39 Suppl 1:9-16.
3. Wolfe F, Sharp JT. Radiographic outcome of recent-onset rheumatoid arthritis: A 19-year study of radiographic progression. *Arthritis Rheum* 1998;41:1571-82.
4. van der Heijde DM, van Riel PL, van Leeuwen MA, van 't Hof MA, van Rijswijk MH, van de Putte LB. Prognostic factors for radiographic damage and physical disability in early rheumatoid arthritis. A prospective follow-up study of 147 patients. *Br J Rheumatol* 1992;31:519-25.
5. Sharp JT, Wolfe F, Mitchell DM, Bloch DA. The progression of erosion and joint space narrowing scores in rheumatoid arthritis during the first twenty-five years of disease. *Arthritis Rheum* 1991;34:660-8.
6. Guidelines for the management of rheumatoid arthritis: 2002 update. *Arthritis Rheum* 2002;46:328-46.
7. Turner RA, Flint KP, Semble EL, Agudelo CA. Clinical evaluation of radiographic progression in rheumatoid arthritis. *Clin Exp Rheumatol* 1990;8:583-6.
8. Guermazi A, Taouli B, Lynch JA, Peterfy CG. Imaging of bone erosion in rheumatoid arthritis. *Semin Musculoskelet Radiol* 2004;8:269-85.
9. Rahmani M, Chegini H, Najafizadeh SR, Azimi M, Habibollahi P, Shakiba M. Detection of bone erosion in early rheumatoid arthritis: Ultrasonography and conventional radiography versus non-contrast magnetic resonance imaging. *Clin Rheumatol* 2010;29:883-91.
10. Ostendorf B, Mattes-Gyorgy K, Reichelt DC, Blondin D, Wirtz A, Lanzman R, et al. Early detection of bony alterations in rheumatoid and erosive arthritis of finger joints with high-resolution single photon emission computed tomography, and differentiation between them. *Skeletal Radiol* 2010;39:55-61.
11. Ostergaard M, Pedersen SJ, Dohn UM. Imaging in rheumatoid arthritis — Status and recent advances for magnetic resonance imaging, ultrasonography, computed tomography and conventional radiography. *Best Pract Res Clin Rheumatol* 2008;22:1019-44.
12. Ostergaard M, Ejbjerg B, Szkudlarek M. Imaging in early rheumatoid arthritis: Roles of magnetic resonance imaging, ultrasonography, conventional radiography and computed tomography. *Best Pract Res Clin Rheumatol* 2005;19:91-116.
13. Dohn U, Ejbjerg BJ, Hasselquist M, Narvestad E, Møller J, Thomsen HS, et al. Detection of bone erosions in rheumatoid arthritis wrist joints with magnetic resonance imaging, computed tomography and radiography. *Arthritis Res Ther* 2008;10:R25.
14. Perry D, Stewart N, Benton N, Robinson E, Yeoman S, Crabbe J, et al. Detection of erosions in the rheumatoid hand; a comparative study of multidetector computerized tomography versus magnetic resonance scanning. *J Rheumatol* 2005;32:256-67.
15. Goldbach-Mansky R, Woodburn J, Yao L, Lipsky PE. Magnetic resonance imaging in the evaluation of bone damage in rheumatoid arthritis: A more precise image or just a more expensive one? *Arthritis Rheum* 2003;48:585-9.
16. Chen TS, Cruess JV 3rd, Ali M, Troum OM. Magnetic resonance imaging is more sensitive than radiographs in detecting change in size of erosions in rheumatoid arthritis. *J Rheumatol* 2006; 33:1957-67.
17. Goldbach-Mansky R, Mahadevan V, Yao L, Lipsky PE. The evaluation of bone damage in rheumatoid arthritis with magnetic resonance imaging. *Clin Exp Rheumatol* 2003;21:S50-S53.
18. Wakefield RJ, Gibbon WW, Conaghan PG, O'Connor P, McGonagle D, Pease C, et al. The value of sonography in the detection of bone erosions in patients with rheumatoid arthritis: A comparison with conventional radiography. *Arthritis Rheum* 2000;43:2762-70.
19. Dohn UM, Ejbjerg BJ, Court-Payen M, Hasselquist M, Narvestad E, Szkudlarek M, et al. Are bone erosions detected by magnetic resonance imaging and ultrasonography true erosions? A comparison with computed tomography in rheumatoid arthritis metacarpophalangeal joints. *Arthritis Res Ther* 2006;8:R110.
20. Dohn UM, Ejbjerg BJ, Hasselquist M, Narvestad E, Court-Payen M, Szkudlarek M, et al. Rheumatoid arthritis bone erosion volumes on CT and MRI: Reliability and correlations with erosion scores on CT, MRI and radiography. *Ann Rheum Dis* 2007;66:1388-92.
21. Alasaarela E, Suramo I, Tervonen O, Lahde S, Takalo R, Hakala M. Evaluation of humeral head erosions in rheumatoid arthritis: A comparison of ultrasonography, magnetic resonance imaging, computed tomography and plain radiography. *Br J Rheumatol* 1998;37:1152-6.
22. Khosla S, Riggs BL, Atkinson EJ, Oberg AL, McDaniel LJ, Holets M, et al. Effects of sex and age on bone microstructure at the ultradistal radius: A population-based noninvasive in vivo assessment. *J Bone Miner Res* 2006;21:124-31.
23. Boutroy S, Bouxsein ML, Munoz F, Delmas PD. In vivo assessment of trabecular bone microarchitecture by high-resolution peripheral quantitative computed tomography. *J Clin Endocrinol Metab* 2005;90:6508-15.
24. Fouque-Aubert A, Boutroy S, Marotte H, Vilaythiou N, Bacchetta J, Miossec P, et al. Assessment of hand bone loss in rheumatoid arthritis by high-resolution peripheral quantitative CT. *Ann Rheum Dis* 2010;69:1671-6.
25. Stach CM, Bauerle M, Englbrecht M, Kronke G, Engelke K, Manger B, et al. Periarticular bone structure in rheumatoid arthritis patients and healthy individuals assessed by high resolution computed tomography. *Arthritis Rheum* 2010;62:330-9.
26. Finzel S, Rech J, Schmidt S, Engelke K, Englbrecht M, Stach C, et al. Repair of bone erosions in rheumatoid arthritis treated with tumour necrosis factor inhibitors is based on bone apposition at the base of the erosion. *Ann Rheum Dis* 2011;70:1587-93.
27. Arnett FC, Edworthy SM, Bloch DA, McShane DJ, Fries JF, Cooper NS, et al. The American Rheumatism Association 1987 revised criteria for the classification of rheumatoid arthritis. *Arthritis Rheum* 1988;31:315-24.
28. MacNeil JA, Boyd SK. Improved reproducibility of high-resolution peripheral quantitative computed tomography for measurement of bone quality. *Med Eng Phys* 2008;30:792-9.
29. Feldkamp LA, Davis LC, Kress JW. Practical cone-beam algorithm. *J Opt Soc Am A* 1984;1:612-9.
30. Li X, Yu A, Virayavanich W, Noworolski SM, Link TM, Imboden J. Quantitative characterization of bone marrow edema pattern in rheumatoid arthritis using 3 Tesla MRI. *J Magn Reson Imaging* 2012;35:211-7.
31. Li XJ, Ma BC, Bolbos RI, Stahl R, Lozano J, Zuo J, et al. Quantitative assessment of bone marrow edema-like lesion and overlying cartilage in knees with osteoarthritis and anterior cruciate ligament tear using MR imaging and spectroscopic imaging at 3 Tesla. *J Magn Reson Imaging* 2008;28:453-61.
32. Burghardt AJ, Link TM, Majumdar S. High-resolution computed tomography for clinical imaging of bone microarchitecture. *Clin Orthop Relat Res* 2011;469:2179-93.
33. Dohn UM, Boonen A, Hetland ML, Hansen MS, Knudsen LS,



- Hansen A, et al. Erosive progression is minimal, but erosion healing rare, in patients with rheumatoid arthritis treated with adalimumab. A 1 year investigator-initiated follow-up study using high-resolution computed tomography as the primary outcome measure. *Ann Rheum Dis* 2009;68:1585-90.
34. McQueen F, Lassere M, Edmonds J, Conaghan P, Peterfy C, Bird P, et al. OMERACT rheumatoid arthritis magnetic resonance imaging studies. Summary of OMERACT 6 MR imaging module. *J Rheumatol* 2003;30:1387-92.
  35. Cyteval C, Miquel A, Hoa D, Daures JP, Mariette X, Combe B. Rheumatoid arthritis of the hand: Monitoring with a simplified MR imaging scoring method-preliminary assessment. *Radiology* 2010;256:863-9.
  36. Crowley AR, Dong J, McHaffie A, Clarke AW, Reeves Q, Williams M, et al. Measuring bone erosion and edema in rheumatoid arthritis: A comparison of manual segmentation and RAMRIS methods. *J Magn Reson Imaging* 2011;33:364-71.
  37. Lassere M, McQueen F, Ostergaard M, Conaghan P, Shnier R, Peterfy C, et al. OMERACT rheumatoid arthritis magnetic resonance imaging studies. Exercise 3: An international multicenter reliability study using the RA-MRI score. *J Rheumatol* 2003;30:1366-75.
  38. Conaghan P, Lassere M, Ostergaard M, Peterfy C, McQueen F, O'Connor P, et al. OMERACT rheumatoid arthritis magnetic resonance imaging studies. Exercise 4: An international multicenter longitudinal study using the RA-MRI score. *J Rheumatol* 2003;30:1376-9.
  39. Bird P, Ejbjerg B, McQueen F, Ostergaard M, Lassere M, Edmonds J. OMERACT rheumatoid arthritis magnetic resonance imaging studies. Exercise 5: An international multicenter reliability study using computerized MRI erosion volume measurements. *J Rheumatol* 2003;30:1380-4.
  40. Jimenez-Boj E, Nöbauer-Huhmann I, Hanslik-Schnabel B, Dorotka R, Wanivenhaus A-H, Kainberger F, et al. Bone erosions and bone marrow edema as defined by magnetic resonance imaging reflect true bone marrow inflammation in rheumatoid arthritis. *Arthritis Rheum* 2007;56:1118-24.
  41. Hetland ML, Stengaard-Pedersen K, Junker P, Ostergaard M, Ejbjerg BJ, Jacobsen S, et al. Radiographic progression and remission rates in early rheumatoid arthritis — MRI bone oedema and anti-CCP predicted radiographic progression in the 5-year extension of the double-blind randomised CIMESTRA trial. *Ann Rheum Dis* 2010;69:1789-95.
  42. Hetland ML, Ejbjerg B, Horslev-Petersen K, Jacobsen S, Vestergaard A, Jurik AG, et al. MRI bone oedema is the strongest predictor of subsequent radiographic progression in early rheumatoid arthritis. Results from a 2-year randomised controlled trial (CIMESTRA). *Ann Rheum Dis* 2009;68:384-90.
  43. Haavardsholm EA, Boyesen P, Ostergaard M, Schildvold A, Kvien TK. Magnetic resonance imaging findings in 84 patients with early rheumatoid arthritis: Bone marrow oedema predicts erosive progression. *Ann Rheum Dis* 2008;67:794-800.
  44. McQueen FM, Benton N, Perry D, Crabbe J, Robinson E, Yeoman S, et al. Bone edema scored on magnetic resonance imaging scans of the dominant carpus at presentation predicts radiographic joint damage of the hands and feet six years later in patients with rheumatoid arthritis. *Arthritis Rheum* 2003;48:1814-27.